Longitudinal collision mitigation via coordinated braking of multiple vehicles using model predictive control

Jian-Qiang Wang[a], Shengbo Eben Li[a,*], Yang Zheng[a] and Xiao-Yun Lu[b]

[a]*The State Key Laboratory of Automotive Safety and Energy, Tsinghua University, Beijing, China*
[b]*PATH, Institute of Transportation Studies, University of California, Berkeley, CA, USA*

Abstract. The vehicular collision can lead to serious casualties and traffic congestions, especially multiple-vehicle collision. Most recent studies mainly focused on collision warning and avoidance strategies for two consecutive vehicles, but only a few on multiple-vehicle situations. This study proposes a coordinated brake control (CBC) strategy for multiple vehicles to minimize the risk of rear-end collision using model predictive control (MPC) framework. The objective is to minimize total impact energy by determining the desired braking force, where the impact energy is defined as the relative kinetic energy for a consecutive pair of vehicles. Under the MPC framework, this problem is further converted to a quadratic programming at each time step for numerical computations. To compare the performance, three other control strategies, i.e. direct brake control (DBC), driver reaction based brake control (DRBC) and linear quadratic regulator (LQR) control are also considered in this paper. The simulation results, in both a typical scenario and a huge number of scenarios under stochastic situations, show that CBC strategy has the best performance among these four strategies. The proposed CBC strategy has the potential to avoid the collision among a group of vehicles, and to mitigate the impact in cases where the collision is unavoidable.

Keywords: Driver assistance systems, longitudinal collision mitigation, model predictive control, multiple vehicles, V2V

1. Introduction

1.1. Background

Road traffic accidents are recognized as a major problem worldwide. In China alone, due to roadway vehicular accidents, the number of fatalities and injuries in 2013 were 58,539 and 213,724, respectively [5]. Among all accidents, approximately 34.3% were comprised of longitudinal (rear-end) collisions on highways. Hence, longitudinal collision warning and avoidance has the potential to avoid or mitigate a large number of collisions, making this a long-standing topic. Many recent studies have focused on different approaches to improve the traffic safety, for instance, accident detection [1,2,13–16,21,31,32], accident analysis and prevention [22,41,42], and R&D of driver assistance systems and autonomous vehicles [7–9,27,29, 36]. Ngoduy et al. built a multi-anticipative macroscopic traffic model to illustrate the influences between vehicles and the importance of a collision system for enhancing traffic safety [29]. Jansson et al. focused on a forward collision avoidance system using active braking [9]. Their research presented a generic method for calculating the risk for rear-end collision by taking into account of measurement uncertainties and driver behaviors. A comprehensive review of collision avoidance systems can be found in [36]. However, most previous research on collision avoidance [7,36] and road safety simulation [41] considered only the nearest two vehicles. This is because the collision avoidance systems were primarily based on on-board sensors (e.g., radar and/or lidar), without inter-vehicle communica-

*Corresponding author: Shengbo Eben Li, The State Key Lab of Automotive Safety and Energy, Tsinghua University, Beijing 100084, China. E-mail: lishbo@tsinghua.edu.cn.

tions. The problem with such systems is that vehicular accidents on highways, particularly under congested conditions, result from the collective behavior of multiple closely spaced vehicles (i.e., a coupled group) in string formation. Therefore, the last vehicle in the formation experiences an accumulated time delay in responding to the behavior of the vehicles in the front.

In fact, a string of coupled vehicles on a highway is more likely to result in multiple-vehicle accidents, which is believed to be one of the detrimental effects of conventional longitudinal collision avoidance systems. With increasing computing and wireless communication abilities, such as Vehicle-to-Vehicle (V2V) [4], the cooperative driver assistance systems (DAS) have the potential to further mitigate this effect [34,39]. The cooperative DAS has a great potential for avoiding such serious accidents or, at least, for minimizing the impact if the collision is unavoidable by simultaneously controlling the braking of multiple vehicles [25]. In V2V systems, the use of Dedicated Short Range Communication (DSRC) or Wireless Access in Vehicular Environments (WAVE) has the overall advantages of extensive network radio communication capabilities that demonstrate low-latency and high throughput, and which is both robust and scalable [12]. Due to these kinds of characteristics, DSRC/WAVE is suitable for basic safety applications, and can be also combined with other on-board sensor systems, such as vehicle on-board sensors (e.g. lidar/radar), precision position systems (e.g. GPS/DGPS), and vehicle state estimation systems (e.g. wheel speed, vehicle velocity, acceleration and yaw rate). In addition, the relative position and speed of vehicles can be obtained and shared by multi-source information fusion or communication [35]. The accuracy of these parameters can meet the requirements for application in connected vehicles [10,39].

The main advantage of the cooperative DAS is its use of wireless communication for information passing to reduce time delays and to compensate for the deficiencies associated with conventional sensors [4,34]. The internal stability and string stability for multiple vehicle following was analyzed in [24,43], which was critical for the practical traffic flow safety. Naus et al. derived a necessary and sufficient frequency-domain condition for vehicle string formation stability and experimented with two vehicles equipped with cooperative adaptive cruise control (CACC) [28]. For heavy-duty trucks, reducing the actuator delay is also critical for control system performance. For the application of such systems, Lu and Hedrick et al. proposed the design of a hydraulic brake for passenger vehicles that di-

rectly used the master cylinder pressure as the control variable [23]. Technologies of this nature can be used as the foundation for implementation of the approach proposed in this study.

1.2. Preview of key results

The objective of this study is to design a coordinated brake control (CBC) strategy to avoid longitudinal collision, or, if impossible to avoid, to mitigate the impact of multiple-vehicle longitudinal collision. The total relative kinetic energy is used as a novel performance minimization index rather than minimizing relative speed or relative distance errors, which has been most often employed in previous studies. Intuitively, a vehicular system of low kinetic energy poses a low risk of damage and is more stable. Hence, we assume that the safety of the multiple coupled vehicles increases with decreasing relative kinetic energy. The use of the total relative kinetic energy facilitates more safety under conditions where coupled vehicular systems are composed of a variety of vehicle masses, which is generally the case under realistic conditions.

The proposed study is different from the concept of the automated platoon, in which all vehicles have automated control capabilities, and are coordinated and organized in a hierarchical automated highway system [24]. This study employs V2V and vehicle control capabilities applicable to current practical highway systems by coordinating on local vehicle behaviors. Therefore, it is necessary to consider the relationship between the coupled vehicle group and its surrounding environment, i.e., those vehicles in the front and rear of the group that cannot be coupled into the system because of the lack of V2V or automated control capability. Under actual traffic conditions, the coupled group is usually heterogeneous rather than homogeneous, and the group is generally comprised of vehicles of different masses, lengths, and braking systems operated by drivers exhibiting a variety of car-following [3,30] and lane-changing behaviors [33]. The heterogeneous nature of a coupled group can seriously affect platoon control [24] and also the capacity of signalized intersections [40]. Some other studies also put a lot attention to heterogeneous issue, e.g. [20,37]. Here, we consider the case of a heterogeneous group of coupled vehicles. To verify the performance of the proposed CBC strategy, three other control strategies: 1) Direct Brake Control (DBC), 2) Driver Reaction based Brake Control (DRBC), and 3) Linear Quadratic Regulator (LQR) control, are also built for simulation studies, and compared with the proposed approach.
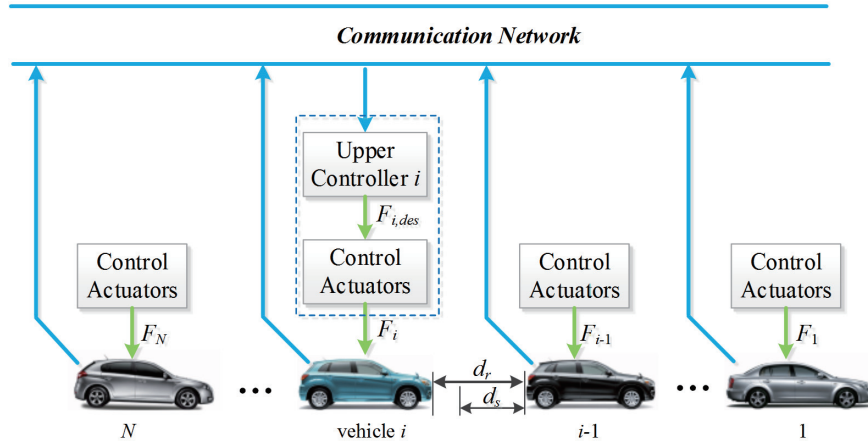
Fig. 1. Overall configuration of multiple vehicle collision mitigation control, where F_i is the actual braking force of the i-th vehicle, $F_{i,des}$ is the desired braking force, d_r is the actual relative distance, and d_s is the safe distance gap.

The main contributions of this study are as follows. (a) Multiple coupled vehicles are directly taken into account rather than considering only two vehicles, as typically done in previous work. (b) The total relative kinetic energy between each consecutive pair of vehicles is used as the objective function for collision avoidance and impact mitigation, and the problem is formulated as an optimal control, which is further simplified as a linear model predictive control (MPC) for future real-time implementation. (c) Simulation is conducted using Matlab, where the vehicle masses of the coupled vehicle group are generated and assigned randomly and the vehicle mass in turn determines vehicle length and deceleration capability according to an empirical formula.

The remainder of this paper is organized as follows. Section 2 presents the system analysis and modeling, and Section 3 presents vehicle longitudinal dynamics. Section 4 is devoted to MPC design depending on the vehicle longitudinal dynamic model. The simulation scenario and analysis are discussed in Section 5, and Section 6 presents concluding remarks.

2. System analysis and modeling

For this study, we consider a system composed of closely following vehicles, i.e. multiple longitudinally coupled vehicles, for collision avoidance and impact mitigation. Adjacent vehicles in a given lane are coupled if their states (speed and distance) jointly satisfy some predefined conditions, i.e., if any longitudinal maneuver of the subject vehicle would require its follower to take immediate action to avoid collision. For standard highway driving, the distance between adjacent vehicles in terms of time according to their speed (time headway (THW)) ranges from 0.7 to 3.8 s [6]. Therefore, most vehicles in car-following scenarios are actually coupled in highway traffic and can be organized into groups. The boundaries among groups depend on several factors, including (1) the type of vehicles involved, (2) the maximum deceleration capability, (3) current speed and THW, (4) traction conditions between the tires and roadway, and (5) wireless communication availability. Wireless communication is critical for coordinated control of braking of each vehicle and for broadcasting the vehicle types and deceleration capabilities of the vehicles of which the group is composed in the message set.

The overall control system for each group of coupled vehicles contains both upper and lower level controls, as shown in Fig. 1. The function of the upper level control is to generate the desired braking force for each vehicle to avoid collision or minimize potential impact if collision is unavoidable. The controller is also subject to several constraints, including the deceleration capabilities of each vehicle. The lower level control activates the brake system to achieve the desired braking force. This study primarily focuses on the upper level control. From a practical viewpoint, each vehicle may have a different powertrain depending on the vehicle type. Most heavy-duty vehicles are equipped with various braking systems, such as pneumatic brakes, engine retarders, and transmission retarders, whereas many passenger cars are equipped with disk or drum brakes, which may be hydraulic or electric. For simplicity of modeling, the differences between vehicle types in a

coupled group are quantified according to the deceleration capability of each vehicle.

As suggested in [17], the collision impact mitigation system is only activated if a certain collision threat threshold is reached. This condition can be determined by sensor detection, risk assessment, and warning the driver. If a driver fails to respond appropriately to the warning of an accident risk, the CBC strategy is activated as the last resort.

To properly define the system, the following assumptions are made.

1) *Assumption 1:* The desired minimum deceleration of the first vehicle and the desired maximum deceleration of the last vehicle in the coupled group are known.
2) *Assumption 2:* Each vehicle has a front-looking and rear-looking radar/lidar to detect intervehicle distance and relative speed reliably.
3) *Assumption 3:* Vehicles in the coupled group can communicate with each other (duplex communication).
4) *Assumption 4:* All vehicles in the coupled group are equipped with devices for controlling the braking force.

2.1. Overall system structure

Figure 1 shows the overall system structure for multiple-vehicle brake control. The system includes remote sensor detection, system state estimation, a DSRC communication network, control and decision making, and control of actuators. The time to collision (TTC) is a critical variable for automatic control. The TTC is refined into the following time point sequences for improved performance in active vehicle safety.

1) *System coupling time:* A group of vehicles in the same lane can be in coupled status for a certain time period denoted as the coupling time.
2) *System warning time:* The driver receives a warning signal before brake activation for passive collision avoidance.
3) *Braking start time t_0:* The CBC actuation starts time necessary to avoid collision if the driver does not appropriately respond to the warning, or, if unavoidable, the earliest time possible to activate the brake for collision active impact mitigation.
4) *Collision start time:* Time instant at which at least one pair of vehicles collides.
5) *Collision end time:* Time instant at which the collision scenario ends.

Here, the magnitude of each period must be quantitatively determined in a reasonable manner. We focus exclusively on the control action by braking beginning at t_0 to the time point when the maneuver (collision avoidance or impact mitigation) is completed. The system considers only coupled vehicles.

2.2. Upper level control strategy

The differences between vehicles include mass, deceleration capability, sensor detection, control actuation, and overall time delay. It is impractical to apply a constant deceleration to each vehicle. Instead, the braking torque of each vehicle must be adjusted according to the current and predicted states on the basis of sensor measurements. The upper level control strategy can be stated as follows.

1) The first vehicle should brake as little as possible to fully use the space in front and to minimize impact with following vehicles. However, the degree of braking is not completely free but is potentially limited by vehicles ahead that are not in the coupled group. Hence, a tradeoff is always made for the first vehicle between reducing the impact with the following vehicle and the risk of collision with those ahead.
2) The last vehicle should apply the brake to the greatest extent possible to fully use its rear space and to minimize its impact to the vehicle in front of it. However, again the degree of braking is not completely free but is potentially limited by vehicles not in the coupled group that are following behind. Hence, a tradeoff is always made for the last vehicle between reducing the impact with the vehicle ahead and the risk of collision with those behind.
3) The desired braking force between all other vehicles will be determined by the current and predicted states of each vehicle, which are estimated according to real-time sensor measurements.
4) State prediction in the finite time horizon of each vehicle is conducted by an MPC approach.

The algorithm for longitudinal collision avoidance and impact minimization should consider the following factors: (1) Multiple-vehicle scenario, (2) mechanical definition of impact, (3) mass of each vehicle, (4) relative distance and relative speed at braking, (5) relative distance and speed at collision, (6) braking capability of each vehicle, (7) braking constraint applied to the first vehicle, and (8) braking constraint applied to the last vehicle.

2.3. Relative kinetic energy

A quantitative description of the multiple-vehicle collision scenario also depends on vehicle types. In these cases, the kinetic energy during collision is not fixed. Moreover, it would be difficult to accurately estimate the collision impact for each pair of vehicles. Therefore, we use the relative kinetic energy before collision as the measure of the potential impact of collision between a pair of vehicles, which in turn is used to estimate the overall system potential impact. This is physically justified because the energy of the collision is the work done by the relative kinetic energy. The following total relative kinetic energy $E(t)$ as a function of time t serves as the integrand of objective function:

$$E(t) = \frac{1}{2} \sum_{i=2}^{N} m_i \left(v_{i-1}(t) - v_i(t) \right)^2, \qquad (1)$$

where v_i and m_i are the velocity and mass of the i-th vehicle, respectively, and N denotes the number of vehicles in the coupled group. Here, the mass of the first vehicle is not considered. As discussed previously, the minimization of the total relative kinetic energy is helpful in reducing the impact of collision when collision is unavoidable.

3. Vehicle longitudinal dynamics model

The vehicle longitudinal dynamics model must consider the powertrain, brake system, aerodynamic drag forces, longitudinal tire forces, rolling resistance forces, and gravitational forces. To obtain a proper model for control law design and analysis, some reasonable assumptions must be stated clearly [18,19].

1) Vehicles are assumed to run on a high-friction road such that the tire slip is negligible; this assumption is reasonable because the usage of such devices as anti-lock brake system (ABS) can limits the tire slip in a small range when braking on a high-friction road. Thus, we neglect the tire slip for controller design.
2) The vehicle is assumed to be a rigid symmetrical body.
3) The pitching and yaw motions of the vehicle body are neglected.
4) The influence of pitch and yaw motions on longitudinal motion is neglected. Though it is true that the pitching motion results in a certain load transfer and may affect the braking performance and

consideration of this factor could yield a more accurate prediction of the braking performance, it would complicate the MPC design. Hence, we neglect the pitching motion to reduce complexity of the controller design.
5) The vehicle moves in a flat plane.

Based on the assumptions above, the longitudinal dynamics for each vehicle in the coupled group are as follows [18]:

$$\begin{cases} \dot{x}_i(t) = v_i(t) \\ \dot{v}_i(t) = \dfrac{1}{m_i} \left(F_i(t) - C_A v_i^2 - m_i gf \right) \end{cases}, \qquad (2)$$
$$i = 1, 2, \ldots, N$$

where $x_i(t)$ is the longitudinal distance with respect to a common inertial coordinate system, C_A is the lumped aerodynamic drag coefficient, is the acceleration due to gravity, f is the coefficient of rolling resistance, and $F_i(t)$ denotes the actual braking force in the longitudinal direction of the i-th vehicle. Because sensors and actuators in mechanical systems have their own inherent dynamics, the actual braking force $F_i(t)$ cannot accurately follow the desired braking force $F_{i,des}(t)$ immediately. Hence, a lumped first-order inertial dynamics between $F_i(t)$ and $F_{i,des}(t)$ is assumed [19]:

$$F_i = \frac{1}{\tau_i s + 1} F_{i,des}, \qquad (3)$$

where τ_i is the time constant of the first-order inertial delay for the i-th vehicle and s is the Laplace operator.

4. MPC control formulation

4.1. Vehicle longitudinal model for control

It is assumed that Δt represents the sampling time for system discretization. The aforementioned dynamics can be discretized into a discrete time model for MPC design as follows:

$$\begin{cases} x_i(k+1) = x_i(k) + v_i(k)\Delta t \\ v_i(k+1) = v_i(k) + \\ \qquad \left(\dfrac{F_i(k)}{m_i} - \dfrac{C_A v_i^2(k)}{m_i} - gf \right) \Delta t \\ F_i(k+1) = \dfrac{\tau_i - \Delta t}{\tau_i} F_i(k) + \\ \qquad \dfrac{\Delta t}{\tau_i} F_{i,des}(k) \end{cases}, \qquad (4)$$

where k represents the time step.

The objective function over the predictive horizon is

$$J(k) = \frac{1}{2} \sum_{j=1}^{N_p} \sum_{i=2}^{N} m_i \tag{5}$$
$$[v_{i-1}(k+j|k) - v_i(k+j|k)]^2,$$

where $*(k+j|k)$ denotes the predicted state at time $k+j$ obtained by starting from the current time k, and N_p denotes the length of the predictive horizon.

The system is constrained according to vehicle deceleration abilities, as expressed in Eq. (6a). In addition, the first vehicle in the front end and the last vehicle in the rear end of the coupled group provide the constraints expressed in Eqs (6b) and (6c). Finally, the coupled group must have the ability to avoid collision, so the constraint in Eq. (6d) is established.

$$a_i^{\min} \leqslant a_i(k+j|k) \leqslant a_i^{\max}, \tag{6a}$$

$$a_1^{\min} \leqslant a_1(k+j|k) \leqslant c_1, \tag{6b}$$

$$c_N \leqslant a_1(k+j|k) \leqslant a_N^{\max}, \tag{6c}$$

$$x_{i-1}(k+j|k) - x_i(k+j|k) \geqslant d_s, \tag{6d}$$

$$i = 1, 2, \ldots, N, j = 0, 1, \ldots, N_p - 1,$$

where, $a_i^{\max}, a_i^{\min}$ are the maximum possible acceleration and maximum possible deceleration; c_1 is the minimum deceleration value of the first vehicle of the coupled group for avoiding collision with a vehicle ahead; c_N is the maximum deceleration value of the last vehicle in the coupled group for avoiding collision with a vehicle behind; and d_s is the safe distance gap.

Hence, we can write the control problem in the following compact form.

$$\min_{F_{des}(k)} J(k) = \frac{1}{2} \sum_{j=1}^{N_p} \sum_{i=2}^{N} m_i [v_{i-1}(k+j|k)$$
$$- v_i(k+j|k)]^2$$

subject to

$$\begin{cases} x_i(k+j+1|k) = x_i(k+j|k) \\ \quad + v_i(k+j|k)\Delta t \\ v_i(k+j+1|k) = v_i(k+j|k) \\ \quad + \left(\dfrac{F_i(k+j|k)}{m_i} - \dfrac{C_A v_i^2(k+j|k)}{m_i} - gf \right)\Delta t \\ F_i(k+j+1|k) = \dfrac{\tau_i - \Delta t}{\tau_i} F_i(k+j|k) \\ \quad + \dfrac{\Delta t}{\tau_i} F_{i,des}(k+j|k) \end{cases} ,$$

$$\tag{7}$$

$$\begin{cases} a_i^{\min} \leqslant a_i(k+j|k) \leqslant a_i^{\max} \\ a_1^{\min} \leqslant a_1(k+j|k) \leqslant c_1 \\ c_N \leqslant a_1(k+j|k) \leqslant a_N^{\max} \\ x_{i-1}(k+j|k) - x_i(k+j|k) \geqslant d_s \end{cases} ,$$

$$i = 1, 2, \ldots, N, \ j = 0, 1, \ldots, N_p - 1,$$

The abovementioned control aims to mitigate the impact of collision, but may not be able to avoid collision completely under some conditions. In some cases, collision is unavoidable and corresponds to the infeasibility of problem Eq. (7). One solution is to set a slack variable in the constraint Eq. (6d), which enables Eq. (6d) to be imposed as a soft constraint. Another method is to use the last control efforts when encountering infeasibility. In our design, constraint violation usually indicates the inevitability of a collision. Hence, we employ the second method.

The solution to the problem given by Eq. (7) is the sequence of input signal $F_{des}(k) = [F_{des}(k|k), \ldots, F_{des}(k+N_p-1|k)] \in \mathbb{R}^{NN_p \times 1}$, where $F_{des}(k+j|k) = [F_{1,des}(k+j|k), \ldots, F_{N,des}(k+j|k)] \in \mathbb{R}^{N \times 1}$, at the current time instant k.

The solution of Eq. (7) minimizes the cost function in Eq. (5) subject to constraints in Eqs (6a) to (6d). Only the first part of the computed optimal control input sequence is applied to the coupled system during the next sampling interval. At the next time step $k+1$, Eq. (7) is resolved over a shifted horizon to utilize the updated information regarding the coupled vehicle state.

4.2. Linear MPC formulation

The nonlinear optimization of Eq. (7) is nontrivial and must be solved numerically. Here, Eq. (7) is linearized with respect to the operating point, and then transformed into a constrained quadratic programming (QP) problem at each control instant. The prediction horizon is 0.1 s; therefore, the model is linearized at the current speed. Such a strategy naturally ensures that vehicle speed is nearly constant over the predictive horizon. Then, the braking force, aerodynamic drag, and rolling resistance can be regarded as a single variable:

$$u_i(k+j|k) = \frac{1}{m_i}(F_i(k+j|k) \tag{8}$$
$$+ C_A v_i^2(k) - m_i gf),$$

where $u_i(k+j|k)$ is the lumped variable.

The corresponding desired control input $u_{i,des}(k + j|k)$ is defined as follows:

$$u_{i,des}(k + j|k) = \frac{1}{m_i}(F_{i,des}(k + j|k) \\ + C_A v_i^2(k) - m_i g f). \quad (9)$$

Then, the system dynamics Eq. (4) in predictive horizon can be rewritten as

$$X_i(k + j + 1|k) = A_i X_i(k + j|k) \\ + B_i u_{i,des}(k + j|k), \quad (10)$$

where

$$X_i(k + j|k) = [x_i(k + j|k), v_i(k + j|k), \\ u_i(k + j|k)]^T,$$

$$A_i = \begin{bmatrix} 1 & \Delta t & \\ & 1 - \dfrac{2C_A v_i(k)}{m_i}\Delta t & \Delta t \\ & & 1 - \dfrac{\Delta t}{\tau_i} \end{bmatrix},$$

$$B_i = \begin{bmatrix} 0 \\ 0 \\ \dfrac{\Delta t}{\tau_i} \end{bmatrix}.$$

This method makes the optimization problem Eq. (7) linear around an operating point and transforms the control force variable $F_{i,des}(k)$ into the control variable $u_{i,des}(k)$, which is easier to handle. Figure 2 illustrates this linearization method. At the current time instant k_i, the velocity $v_i(k_i)$ holds the same value during the predictive horizon $k_i + 1 \sim k_i + N_p$, and the velocity changes to $v_i(k_i + 1)$ at the next sample time.

Equation (10) is suitable only for single vehicle dynamics. For the coupled group involving N vehicles, we choose the following state vector and control vector.

$$X(k + j|k) = \begin{bmatrix} X_1(k + j|k) \\ X_2(k + j|k) \\ X_3(k + j|k) \\ \vdots \\ X_N(k + j|k) \end{bmatrix} \in \mathbb{R}^{3N \times 1},$$

$$u_{des}(k + j|k) = \begin{bmatrix} u_{1,des}(k + j|k) \\ u_{2,des}(k + j|k) \\ u_{3,des}(k + j|k) \\ \vdots \\ u_{N,des}(k + j|k) \end{bmatrix} \in \mathbb{R}^{N \times 1}.$$
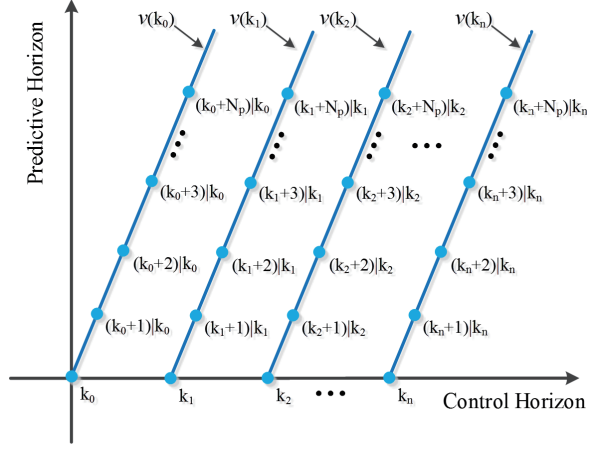

Fig. 2. Diagram of the linearization method.

Then, all vehicle dynamics during the predictive horizon can be written in the following compact form:

$$X(k + j + 1|k) = AX(k + j|k) \\ + Bu_{des}(k + j|k), \quad (11)$$

where

$$A = \begin{bmatrix} A_1 & & & \\ & A_2 & & \\ & & \ddots & \\ & & & A_N \end{bmatrix} \in \mathbb{R}^{3N \times 3N},$$

$$B = \begin{bmatrix} B_1 & & & \\ & B_2 & & \\ & & \ddots & \\ & & & B_N \end{bmatrix} \in \mathbb{R}^{3N \times 3N}.$$

Therefore, we can reduce Eq. (7) into the optimization problem given by Eq. (12) shown below.

$$\min_{u_{des}(k)} J(k) = \frac{1}{2} \sum_{j=1}^{N_p} X^T(k+j|k) \cdot Q \cdot X(k+j|k)$$

subject to

$$X(k+j+1|k) = AX(k+j|k) + Bu_{des}(k+j|k),$$

$$\begin{cases} a_i^{\min} \leqslant a_i(k + j|k) \leqslant a_i^{\max} \\ a_1^{\min} \leqslant a_1(k + j|k) \leqslant c_1 \\ c_N \leqslant a_1(k + j|k) \leqslant a_N^{\max} \\ x_{i-1}(k + j|k) - x_i(k + j|k) \geqslant d_s \end{cases}, \quad (12)$$

$$i = 1, 2, \ldots, N, \;\; j = 0, 1, \ldots, N_p - 1.$$

Here, Q has the appropriate value and dimension. Moreover, Eq. (12) has a quadratic optimal target term and linear constraints. Hence, Eq. (12) can be recast as the constrained QP problem given by Eq. (13).

$$\min_{U} J(k) = \frac{1}{2} U^T H U + P^T U + C$$

$$\text{subject to } A_{con} U \leqslant b_{con}. \tag{13}$$

Here, $U, H, P, C, A_{con}, b_{con}$ have appropriate values and dimensions. Model Eq. (12) is linearized around an operating point. Therefore, the linear time-invariant model Eq. (12) at time k is used to predict the coupled group state $X(k+j|k), j = 0, 1, \ldots, N_p - 1$ in the predictive horizon. Accordingly, the optimization variables $u_{des}(k|k)$ are used to solve the braking force $F_{i,des}(k|k)$ for each vehicle during the braking process.

4.3. MPC algorithm in implementation

For numerical calculation, it is suggested to sequentially perform the following steps.

Step 1: Initialize $X(k)$ according to sensor measurements and communication to predict the forward N_p time steps.

Step 2: Find the optimal desired braking force $F_{des}(k|k)$ numerically using the QP method.

Step 3: Apply the control (desired braking force) $F_{des}(k|k)$ to the system and then generate the system state of the next time step.

Step 4: If the speed of each vehicle is not reduced to zero, estimate the system state to obtain $X(k+1)$ according to sensor detection.

Step 5: Set $k := k + 1; X(k) = X(k+1)$, and go to Step 2.

5. Simulation and analysis

The coupled group must allow for different types of vehicles because the control algorithm is designed for practical coordination of multi-vehicle longitudinal collision mitigation. Vehicle types are characterized by parameters such as vehicle mass, body length, dynamics of the braking system, and deceleration capability. To verify the performance of the proposed CBC strategy, three other control strategies, namely, Direct Brake Control (DBC), 2) Driver-Reaction based Brake Control (DRBC) and 3) Linear Quadratic Regulator (LQR) control, are simulated for comparison with the proposed strategy. Three strategies are defined as follows.

A. Coordinated brake control (CBC)

CBC coordinates the braking force for each vehicle using MPC, which is formulated into a constrained QP problem. The design details of CBC have been given in Sections 3 and 4.

B. Direct brake control (DBC)

DBC employs equivalent assumptions and conditions as CBC. Vehicles in the coupled group must have V2V communication and automatic braking capabilities. The difference between DBC and CBC is that DBC directly employs the full deceleration ability of each vehicle rather than coordinating the braking force for each vehicle under emergency conditions. Therefore, each vehicle in the coupled group immediately and fully employs braking when confronting critical events.

C. Driver-reaction based brake control (DRBC)

DRBC does not assume that vehicles in the coupled group have V2V communication and automatic braking capabilities. Only the driver judges the driving situation and brakes the vehicle fully after a certain driver reaction time for emergency situations.

D. Linear quadratic regulator control (LQR) control

This method employs LQR control during braking, which is a classical optimal control strategy for Cooperative Adaptive Cruise Control (CACC) during normal driving conditions. In this study, the constant THW policy is used for the car-following model, and the control objective is to follow the driver's desired spacing (see [26] for more details).

5.1. Simulation parameters

Vehicles with large masses are usually also long and have limited deceleration capabilities. Here, the mass of each vehicle is generated randomly and is used to determine both the vehicle body length and deceleration capability. The minimum mass used is $M_{\min} = 1000$ kg (passenger car), and the maximum mass is $M_{\max} = 15000$ kg (half-loaded heavy-duty truck). For a given number of vehicles N, the mass of each vehicle is randomly generated as follows.

$$m_i = M_{\min} + (M_{\max} - M_{\min}) \cdot rand(1),$$
$$i = 1, 2, \ldots, N. \tag{14}$$

Then, the vehicle body length is determined as follows:

$$L_i = 3.0(1-\alpha)+23.0\alpha, \alpha = \frac{m_i - M_{\min}}{M_{\max}}. \quad (15)$$

As such, the minimum body length is 3.0 m (passenger car) and maximum body length is 23 m (heavy-duty truck: tractor – trailer combination). Li et al. determined that the time constant for the braking system of a typical heavy-duty truck is about 0.45 s [19]. For simplicity, we assume that large vehicles have large time constants for their braking systems. Hence, the time constant for a vehicle braking system is given by the following.

$$\tau_i = 0.2\left(1-\alpha\right) + 0.6\alpha, \alpha = \frac{m_i - M_{\min}}{M_{\max}}, \quad (16)$$

The vehicle deceleration capability is determined by the following expression.

$$a_i^{\min} = -3.0\left(2.2 - \frac{m_i}{15000}\right), i = 1, 2, \ldots, N. \quad (17)$$

Employing the THW policy, the car-following distance distribution is obtained in the coupled group. The THW is between 0.7 s to 3.8 s in 90% of the cases on highways in China [6]. In the present study, the THW distribution was made to follow the Gaussian distribution $THW \sim N(1.5, 0.1^2)$. Johansson et al. pointed out that the driver reaction time to warning signals is spread over a period of 0.3 s to 2 s, and the average driver reaction time is 0.66 s [11]. Here, the driver reaction time was made to obey the Gaussian distribution $T_d \sim N\left(0.66, 0.1^2\right)$ during simulation scenarios.

5.2. Typical scenario simulation

Typical scenario simulation results using the aforementioned four control strategies are discussed in this section. It is assumed that the simulation scenario involves nine vehicles. The prediction time period and control time period are all 5 steps, and the length of the time step used for the simulation is 0.02 s. The initial speed of each vehicle is 31 m/s plus ± 10% and is made to fluctuate randomly.

The minimum deceleration of the leading vehicle is limited to 100% of its maximum deceleration capability ($c_1 = -4.87$ m/s^2), indicating that the first vehicle in the coupled group needs to apply full braking to

Table 1
Vehicle parameters used in the simulation

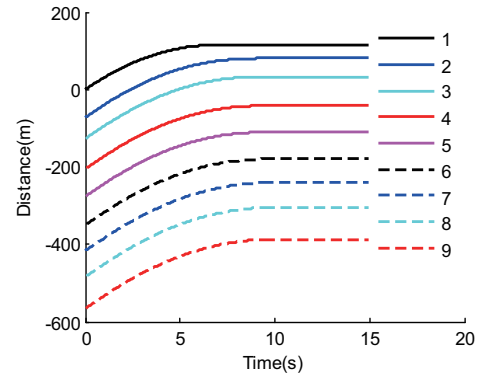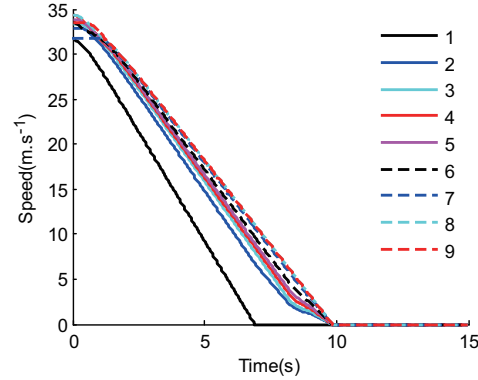| Id	m ($\times 10^3$ kg)	$-a^{\min}$ (m/s^2)	L (m)	THW	T_d (s)	τ
1	8.66	4.87	13.95	1.57	0.73	0.42
2	2.38	6.12	4.97	1.63	0.63	0.24
3	12.45	4.11	19.35	1.35	0.74	0.53
4	9.62	4.68	15.32	1.57	0.62	0.45
5	11.99	4.20	18.71	1.49	0.77	0.51
6	7.50	5.10	12.28	1.49	0.57	0.39
7	5.31	5.54	9.15	1.52	0.61	0.32
8	14.23	3.75	21.90	1.58	0.70	0.58
9	7.43	5.11	12.18	1.65	0.56	0.38

Fig. 3. Nine vehicle trajectories by CBC.

Fig. 4. Nine vehicle speed profiles by CBC.

avoid accidents with vehicles in front of the coupled group. The maximum deceleration of the last vehicle is limited to 92% of its maximum deceleration capability ($c_N = -4.71$ m/s^2), indicating a potential collision threat to the last vehicle in the coupled group with a vehicle following behind. The distribution of mass, deceleration capability, THW, driver reaction time, and time constant for the vehicle braking system are listed in Table 1.

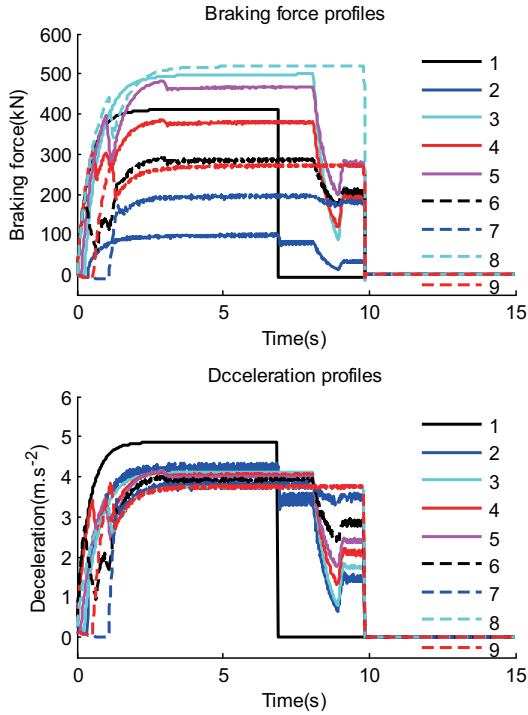For the CBC strategy, the corresponding trajectories and speed profiles are illustrated in Figs 3 and 4, re-

Fig. 5. Nine vehicle braking force profiles and deceleration profiles by CBC.

spectively. The braking force and deceleration profiles are shown in Fig. 5. The simulation results demonstrate collision avoidance for all vehicles. From Figs 3 and 4, it can be seen that, after about 10 s, all the vehicles stopped when employing the CBC strategy and all the inter-vehicle distances remained greater than a certain value during the braking process. This indicates that collision was completely avoided although vehicles were present in front of and behind the coupled system. As stated above, the vehicles in front of and behind the system are represented by the constraints of the minimum deceleration of the leading vehicle and the maximum deceleration of the last vehicle in the coupled group, respectively. Figures 3 and 4 indicate that the CBC strategy can not only regulate the relative speed but also maintain the inter-vehicle distance within a reasonable range.

Although the initial speeds of the vehicles appear to be random, their speeds become regular after several seconds using the CBC strategy, as shown in Fig. 4. The optimization function (1) seeks to minimize the total relative kinetic energy of the coupled group, which is equivalent to reducing the relative speeds of all vehicles to as close to zero as possible. If all the vehicles are identical, the relative speeds of all vehicles' speed
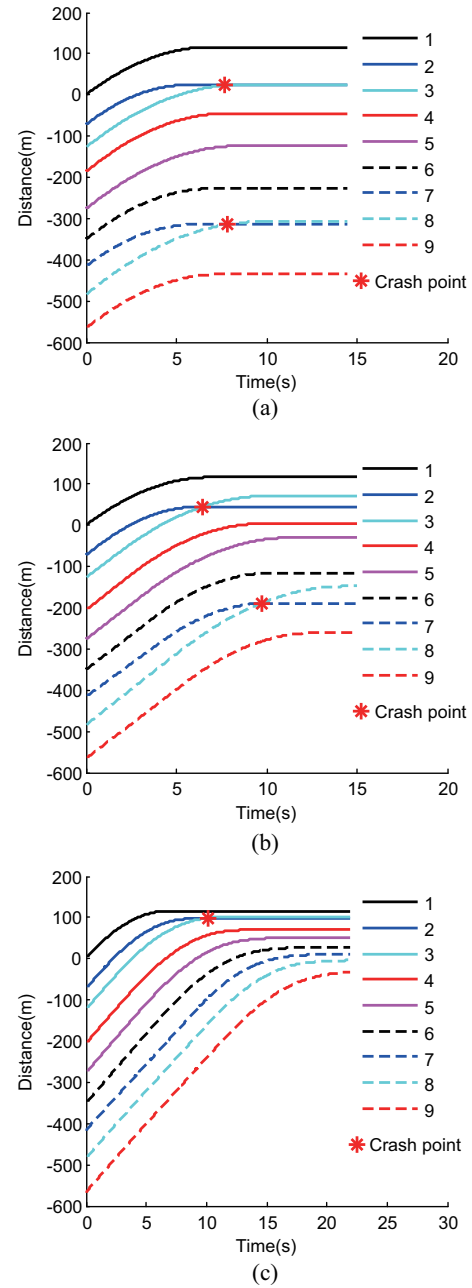

Fig. 6. Nine vehicle trajectories by (a) DBC, (b) DRBC, and (c) LQR.

can be controlled into no difference, which means that vehicles in the coupled group can be effectively treated as a single, enlarged vehicle. Figures 6(a)–(c) demonstrate the respective vehicle trajectories generated by DBC, DRBC, and LQR under equivalent conditions.

It can be observed from Fig. 6(a) that two vehicular accidents occurred between vehicles 2 and 3, and
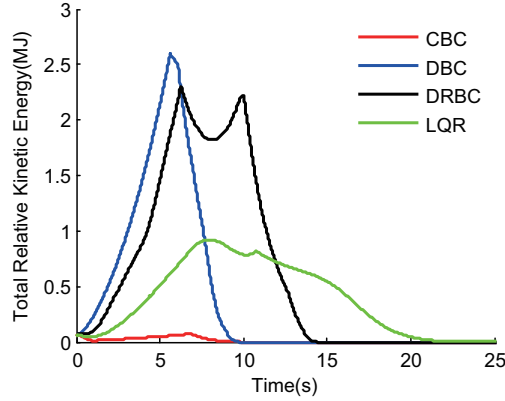
Fig. 7. Comparison of the total relative kinetic energies produced by the four control strategies over the entire braking process.

between vehicles 7 and 8 using the DBC strategy. From Table 1, we can see that vehicles 2 and 7 have good deceleration capabilities ($a_{min2} = -6.12$ m/s^2 and $a_{min7} = -5.54$ m/s^2). Vehicles 2 and 7 stopped within 100 m and 110 m, respectively. However, vehicles 3 and 8 have relatively poor deceleration capabilities ($a_{min3} = -4.10$ m/s^2 and $a_{min8} = -3.75$ m/s^2). Vehicle 3 requires over 150 m to stop fully and vehicle 7 requires over 170 m. The difference between these two stop distances is larger than the car-following distance. Hence, collision occurred between these vehicles. As shown in Fig. 6(b), two accidents between vehicles 2 and 3, and between vehicles 7 and 8 occurred using the DRBC strategy. The differences of the deceleration capabilities between vehicles are the cause of collision in this case. The driver reaction time is another major factor. The driver's response time causes much more serious collisions using this strategy relative to using the DBC strategy (i.e., the collision speed is higher using the DRBC strategy). In Fig. 6(c), it can be seen that vehicle 3 collided with vehicle 2 under LQR control.

Figure 7 shows a comparison of the relative kinetic energies produced by the aforementioned four braking control strategies during the braking process. It should be noted that Fig. 7 is only a schematic because we have disregarded collisions during the simulation process. The proposed CBC strategy achieves the lowest relative kinetic energy among these strategies over the entire braking process.

5.3. Multi-simulation result

To test the performance of the CBC strategy under different conditions, we ran 1000 simulations while
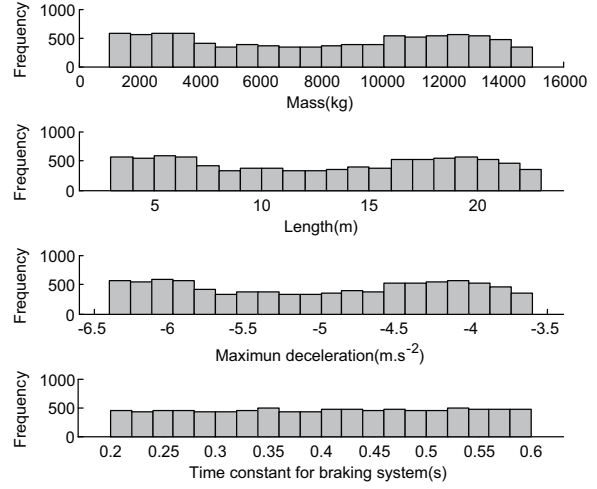

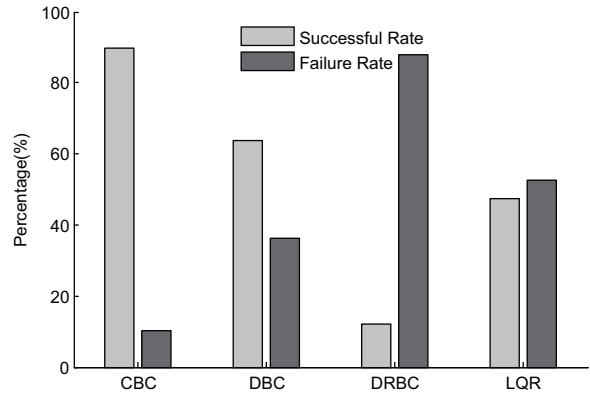Fig. 8. Vehicle attribute distributions for 1000 simulations.

Fig. 9. Success and failure rates on the basis of complete avoidance of collision for the four control strategies.

randomly generating certain parameters. The initial parameter selection for each round of simulation is same as described in previous section.

Figure 8 shows the vehicle attribute distributions for the 1000 simulations. To make the conditions more hazardous, we added one small vehicle, whose mass was randomly generated in the range 1000–3000 kg and one large vehicle, whose mass was randomly generated in the range 10000–15000 kg in each simulation. The positions of these two vehicles were randomly placed in the coupled group with the constraint that the large vehicle at the behind the small vehicle.

Figure 9 shows the success and failure rates on the basis of complete avoidance of collision using the four strategies. During the 1000 simulations, collision was completely avoided in 898 simulations (89.8%) using the CBC strategy. When employing DBC, DRBC, and

Table 2
Failure rates of the control strategies under the various simulation
conditions resulting in collision

Different strategies	Failure cases	Failure rate in collision cases			
		CBC	DBC	DRBC	LQR
CBC	102	100%	73.5%	99.0%	99.0%
DBC	364	20.6%	100%	100%	65.1%
DRBC	881	11.5%	41.3%	100%	55.7%
LQR	527	19.17%	44.97%	93.17%	100%

LQR control, the successful rates were reduced from 89.8% to 63.6%, 11.9%, and 47.3%, respectively. Figure 10 shows box plots of the statistical data of the 1000 simulations using the four control strategies for the case of failure (Figs 10(a) and (b)) and for the case of success (Figs 10(c) and (d)). As shown in Figs 10(c) and (d), among the successful braking cases, the maximum relative kinetic energy for the proposed CBC strategy is the smallest, and the minimum relative distance is the largest during the braking process relative to the other three strategies. As such, when the collision is unavoidable, the collision impact for the CBC strategy is the lowest (Figs 10(a) and (b)). Therefore, we can claim that the proposed CBC strategy demonstrates the best performance for collision avoidance among the four control strategies considered. On the other hand, LQR control for CACC demonstrates good performance under normal conditions [26]. However, LQR control provides degraded performance for collision avoidance under certain emergency conditions.

As shown in Table 2, for the 102 failed simulations using the CBC strategy, the failure rates of DBC, DRBC, and LQR under equivalent conditions were 73.53%, 99.02%, and 99.02%, respectively. For the 364 failure cases using DBC, the failure rates of CBC, DRBC, and LQR were 20.6%, 100%, and 65.11%, respectively. The statistical data in Table 2 also verifies that the proposed CBC strategy demonstrates the best performance.

5.4. Discussions on unavoidable collision

Intuitively, a collision will occur between two vehicles in the coupled group if a vehicle has good deceleration ability, but its following vehicle has poor deceleration ability. A vehicle with poor deceleration ability is usually a large vehicle (e.g., heavy-duty truck), and a vehicle with good deceleration ability is usually a small vehicle (e.g., passenger car). A large vehicle requires a long distance to stop, whereas a small vehicle can stop completely within a short distance. Therefore, if a large vehicle follows a small vehicle without a suf-
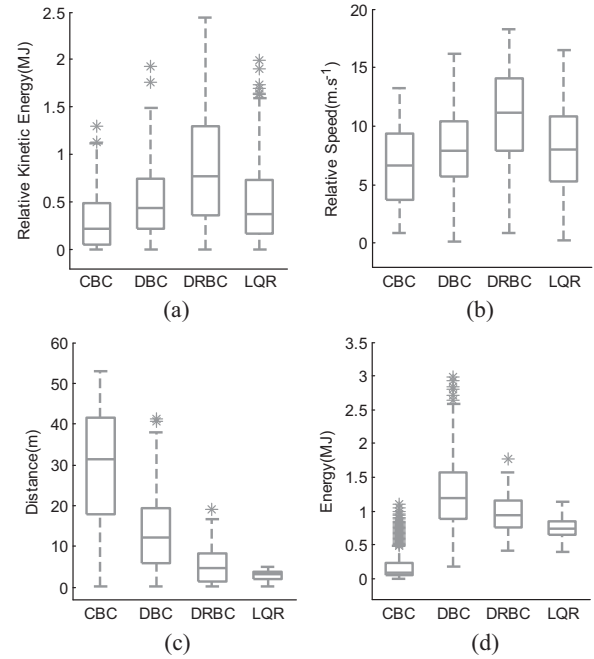

Fig. 10. Box plots of the statistical data of 1000 simulations using the four control strategies. (a) Relative kinetic energy and (b) relative speed distributions in the case of failure. (c) Minimum relative distance and (d) maximum relative kinetic energy in the case of success. Note that the number of failures is CBC: 102, DBC: 364, DRBC: 881, and LQR: 527.
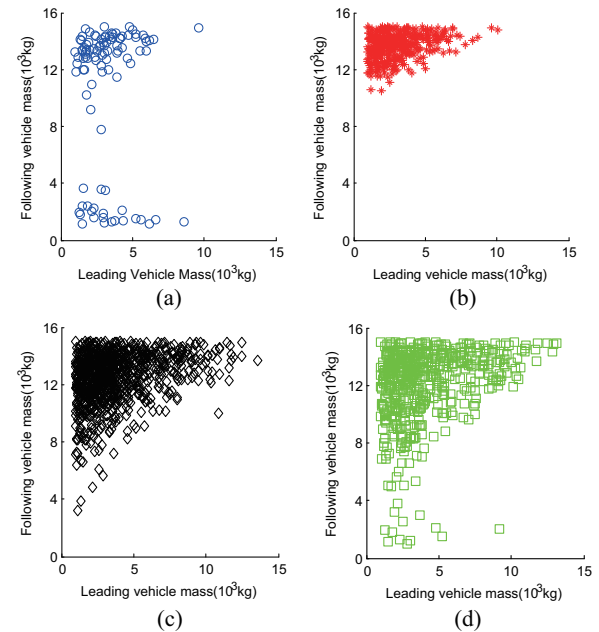

Fig. 11. Collision vehicle types for collision cases of (a) CBC, (b) DBC, (c) DRBC, and (d) LQR.

Table 3
Success rate for collision avoidance under different mass distribution ranges*

	CBC	DBC	DRBC	LQR
Case 1	100%	98%	81.8%	75%
Case 2	100%	99.6%	59.8%	83.4%

*Note. Case 1: Vehicle masses generated between 1000 kg and 5000 kg; Case 2: Vehicle masses genrated between 10000 kg and 15000 kg. Each case is based on 500 simulations.

ficient distance between them, a collision may be unavoidable regardless of the control strategy employed.

A possible solution for collision avoidance involving a large vehicle is to increase the car-following distance or reduce the driving speed. Using the simulation results in the previous section, the distributions of collision vehicle types can be obtained (see Fig. 11). It can be observed that the majority of collision cases occurred between a large vehicle and a small vehicle, and that the proposed CBC strategy can reduce the collision probability between large and small vehicles. However, doing so may result in the collision between small vehicles because the collision impact (relative kinetic energy) between small vehicles is typically smaller than for the case when large vehicles are involved. Hence, from this viewpoint, the proposed CBC strategy has good performance and enhances overall safety.

The mass distribution (or deceleration capability distribution) in the coupled group has a significant influence on the success rate of collision avoidance. If we alter the simulation parameter to make the vehicle mass distribution follow a narrow range, thereby producing a more homogeneous coupled group, the success rate of all four control strategies are substantially improved, as demonstrated in Table 3. In this case, the coupled group can be treated as one extended vehicle, and collision is usually avoided.

6. Conclusions

This study considers the cooperative braking control (CBC) strategy for a group of vehicles with the purpose of minimizing the risk of rear-end collision. The upper level controller is designed using model predictive control (MPC) theory, in which the total relative kinetic energy between consecutive pairs of vehicles is used as the cost function. This cost function is able to generate the desired braking force for each vehicle in the coupled group required to avoid collision or to minimize the total impact if collision is unavoidable.

The MPC is reduced to a constrained QP problem for faster computation. The algorithm can be implemented in a centralized or decentralized scheme. To be implemented as a centralized scheme, one vehicle in the coupled group must act as the coordinator to calculate the desired deceleration for each vehicle and communicate it in real time. For a decentralized scheme, each vehicle must calculate and activate its desired deceleration independently. Three other control strategies, namely DBC, DRBC, and LQR, are built for fair comparison with CBC. The findings include.

(1) In the absence of a minimum deceleration limit for the first vehicle and a maximum deceleration limit for the last vehicle in the coupled group, it is likely that most collisions could be avoided using the proposed braking control. However, in practice, the coupled group cannot be completely isolated from other vehicles in front of and behind the coupled group.

(2) Intuitively, a system with less kinetic energy will have a reduced risk to safety and be more stable. The control objective in the proposed strategy is to minimize the total relative kinetic energy. The extensive simulation results verify the effectiveness of the proposed strategy. The reduced relative kinetic energy leads to reduced risk of collision.

(3) Heterogeneous braking capabilities are a major cause of collisions. The multi-simulation results show that unavoidable collisions often occur among vehicles that follow a smaller leader in the coupled group, because large vehicles typically require a longer distance to stop relative to small vehicles. A possible solution for collision avoidance is to increase the car-following distance or reduce the driving speed.

There are still a few open questions in the framework of cooperative braking control. Future work will include how to implement the proposed strategy with passenger cars and/or trucks, and how to implement wireless connection technology and enhance automatic brake control capabilities for various environmental conditions.

References

[1] H. Adeli and A. Karim, Wavelets in intelligent transportation systems, *John Wiley and Sons*, West Sussex, United Kingdom, 2005.

[2] H. Adeli and A. Karim, Fuzzy-wavelet RBFNN model for freeway incident detection, *Journal of Transportation Engineering, ASCE* **126**(6) (2000), 464–471.

[3] K. Aghabayk, N. Forouzideh and W. Young, Exploring a local linear model tree approach to car-following, *Computer-Aided Civil and Infrastructure Engineering* **28**(8) (2013), 581–593.

[4] S. Biswas, R. Tatchikou and F. Dion, Vehicle-to-vehicle wireless communication protocols for enhancing highway traffic safety, *IEEE Communications Magazine*, (2006), 74–82

[5] DTM-China (Department of Traffic Management-China), Annual report of road traffic accidents statistics in P.R. China, Scientific Research Institute of Traffic Management, Ministry of Public Security, Beijing, 2013.

[6] R.N. Dang, F. Zhang, T. Yasuhiko, W. Chu and K. Li, Braking characteristics of Chinese driver in highway and urban road, *7th IFAC Symposium on Advances in Automotive Control*, (2013), 322–327.

[7] R. Domínguez, J. Alonso, E. Onieva and C. González, A transferable belief model applied to LIDAR perception for autonomous vehicles, *Integrated Computer-Aided Engineering* **20**(3) (2013), 289–302.

[8] R. Haijema and E.M.T. Hendrix, Traffic responsive control of intersections with predicted arrival times: A markovian approach, *Computer-Aided Civil and Infrastructure Engineering* **29**(2) (2014), 123–139.

[9] J. Jansson, J. Johansson and F. Gustafsson, Decision making for collision avoidance systems, *Society of Automotive Engineering SAE*, (2002-01), 0403.

[10] F. Jimeᷧnez, J. Naranjo, F. Garcia and J. Armingol, Can low-cost road vehicles positioning systems fulfil accuracy specifications of new ADAS applications? *The Journal of Navigation* **64** (2011), 251–264.

[11] G. Johansson and K. Rumar, Drivers' brake reaction times, *Human Factors: The Journal of the Human Factors and Ergonomics Society* **13**(1) (1971), 23–27.

[12] G. Karagiannis, O. Altintas and E. Ekici, Vehicular networking: A survey and tutorial on requirements, architectures, challenges, standards and solutions, *Communications Surveys & Tutorials, IEEE* **13**(4) (2011), 584–616.

[13] A. Karim and H. Adeli, CBR model for freeway work zone traffic management, *Journal of Transportation Engineering, ASCE* **129**(2) (2003), 134–145.

[14] A. Karim and H. Adeli, Comparison of the fuzzy – wavelet RBFNN freeway incident detection model with the california algorithm, *Journal of Transportation Engineering, ASCE* **128**(1) (2002), 21–30.

[15] A. Karim and H. Adeli, Fast automatic incident detection on urban and rural freeways using wavelet energy algorithm, *Journal of Transportation Engineering, ASCE* **129**(1) (2003), 57–68.

[16] A. Karim and H. Adeli, Incident detection algorithm using wavelet energy representation of traffic patterns, *Journal of Transportation Engineering, ASCE* **128**(3) (2002), 232–242.

[17] K. Lee and H. Peng, Evaluation of automotive forward collision warning and collision avoidance algorithms, *Vehicle System Dynamics* **43**(10) (2005), 735–751.

[18] S.E. Li and H. Peng, Optimal strategies to minimize fuel consumption of passenger cars during car-following scenarios, *Journal of Automobile Engineering* **226**(3) (2012), 419–429.

[19] S Li., K. Li, R. Rajamani and J. Wang, Model predictive multi-objective vehicular adaptive cruise control, *Control Systems Technology, IEEE Transactions on* **19**(3) (2011), 556–566.

[20] X. Li, F. He, X. Cai, D. Zhang and Y. Chen, A method for topological entity matching in the integration of heterogeneous CAD systems, *Integrated Computer-Aided Engineering* **20**(1) (2013), 15–30.

[21] Y. Liu, J. Yu, P. Li and K. Wehner, A generalized integrated corridor diversion control model for freeway incident management, *Computer-Aided Civil and Infrastructure Engineering* **28**(8) (2013), 604–620.

[22] G. Lu and C. Bo, Relationship between road traffic accidents and conflicts recorded by drive recorders, *Traffic Injury Prevention* **12** (2011), 320–326

[23] X. Lu and J. Hedrick, Longitudinal control design and experiment for heavy-duty trucks, *In American Control Conference, 2003. Proceedings of the 2003*.

[24] X. Lu and J. Hedrick, Practical string stability for longitudinal control of automated vehicles, *Vehicle System Dynamics* **41** (2004), 577–586.

[25] F.J. Martinez, C.K. Toh, J.C. Cano C.T. Calafate and P. Manzoni, Emergency services in future intelligent transportation systems based on vehicular communication networks, *Intelligent Transportation Systems Magazine, IEEE* **2**(2) (2010), 6–20.

[26] F. Morbidi, P. Colaneri and T. Stanger, Decentralized optimal control of a car platoon with guaranteed string stability, in: *Control Conference (ECC) European*, (2013).

[27] F.A. Moreno J. Gonzalez-Jimenez, J. Blanco and A. Esteban, An instrumented vehicle for efficient and accurate 3D mapping of roads, *Computer-Aided Civil and Infrastructure Engineering* **28**(6) (2013), 403–419.

[28] G.J. Naus, R.P. Vugts, J. Ploeg, M. Van de Molengraft and M. Steinbuch, String-stable CACC design and experimental validation: A frequency-domain approach, *Vehicular Technology, IEEE Transactions on* **59**(9) (2010), 4268–4279.

[29] D. Ngoduy and R.E. Wilson, Multi-anticipative non-local macroscopic traffic model, *Computer-Aided Civil and Infrastructure Engineering* **29**(4) (2014), 248–263.

[30] S. Ossen and S. Hoogendoorn, Heterogeneity in car-following behavior: Theory and empirics, *Transportation Research Part C: Emerging Technologies* **19**(2) (2011), 182–195.

[31] A. Samant and H. Adeli, Enhancing neural network incident detection algorithms using wavelets, *Computer-Aided Civil and Infrastructure Engineering* **16**(4) (2001), 239–245.

[32] A. Samant and H. Adeli, Feature extraction for traffic incident detection using wavelet transform and linear discriminant analysis, *Computer-Aided Civil and Infrastructure Engineering* **15**(4) (2000), 241–250.

[33] D.J. Sun and L. Elefteriadou, Lane – changing behavior on urban streets: An "in-vehicle" field experiment-based study, *Computer-Aided Civil and Infrastructure Engineering* **27**(7) (2012), 525–542.

[34] T. Taleb, A. Benslimane and K. Letaief, Toward an effective risk-conscious and collaborative vehicular collision avoidance system, *IEEE Transactions on Vehicular Technology* **59**(3) (2010), 1474–1486.

[35] R. Toledo-Moreo and A. Zamora-Izquierdo, Collision avoidance support in roads with lateral and longitudinal maneuver prediction by fusing GPS/IMU and digital maps, *Transportation Research Part C* **18** (2010), 611–625.

[36] A. Vahidi and A. Eskandarian, Research advances in intelligent collision avoidance and adaptive cruise control, *Intel-*

ligent Transportation Systems, IEEE Transactions on **4**(3) (2003), 143–153.

[37] D., E. Vega, Medina, R. Messeguer, D. Royo, F. Freitag, S.F. Ochoa and J.A. Pino, Sharing hardware resources in heterogeneous computer-supported collaboration scenarios, *Integrated Computer-Aided Engineering* **20**(1) (2013), 59–77.

[38] J. Wang, D. Ni and K. Li, RFID-based vehicle positioning and its applications in connected vehicles, *Sensors* **14** (2014), 4225–4238.

[39] J. Wang, D. Zhang, J. Liu, M. Lu and K. Li, Multi-objective driving assistance system for intersection support, in: *13th International IEEE Conference on Intelligent Transportation Systems* Madeira, (2010), 348–353.

[40] S.S. Washburn and C.O. CruzCasas, Impact of trucks on sig-

nalized intersection capacity, *Computer – Aided Civil and Infrastructure Engineering* **25**(6) (2010), 452–467.

[41] W. Young, A. Sobhani, M.G. Lenne and M. Sarvi, Simulation of safety: A review of the state of the art in road safety simulation modelling, *Accident Analysis and Prevention* **66** (2014), 89–103.

[42] Y. Zheng, J. Wang, X. Li, C. Yu, K. Kodaka and K. Li, Driving risk assessment using cluster analysis based on naturalistic driving data, in: *IEEE 17th International Conference on Intelligent Transportation Systems, IEEE* (2014), 2584–2589.

[43] Y. Zheng, S. Eben Li, J. Wang, L. Wang and K. Li, Influence of information flow topology on closed-loop stability of vehicle platoon with rigid formation, *17th Intelligent Transportation System Conference, IEEE*, (2014), 2094–2100.